PHOTONICS Research

Generation of optical Fock and W states with single-atom-based bright quantum scissors

ZIV AQUA,[1] M. S. KIM,[2] AND BARAK DAYAN[1,*]

[1]*AMOS and Department of Chemical and Biological Physics, Weizmann Institute of Science, Rehovot 76100, Israel*
[2]*QOLS, Blackett Laboratory, Imperial College London, London SW7 2AZ, UK*
Corresponding author: barak.dayan@weizmann.ac.il

We introduce a multi-step protocol for optical quantum state engineering that performs as "bright quantum scissors," namely truncates an arbitrary input quantum state to have at least a certain number of photons. The protocol exploits single-photon pulses and is based on the effect of single-photon Raman interaction, which is implemented with a single three-level Λ system (e.g., a single atom) Purcell-enhanced by a single-sided cavity. A single step of the protocol realizes the inverse of the bosonic annihilation operator. Multiple iterations of the protocol can be used to deterministically generate a chain of single photons in a W state. Alternatively, upon appropriate heralding, the protocol can be used to generate Fock-state optical pulses. This protocol could serve as a useful and versatile building block for the generation of advanced optical quantum states that are vital for quantum communication, distributed quantum information processing, and all-optical quantum computing. © 2019 Chinese Laser Press

https://doi.org/10.1364/PRJ.7.000A45

1. INTRODUCTION

The field of quantum state engineering (QSE) aims at preparing arbitrary quantum states. Nonclassical states are highly sought after both as a means to test fundamental questions in quantum mechanics [1], as well as a source for various applications in quantum information [2,3], sensing and metrology [4]. Controlling and manipulating the quantum state of optical fields is of particular interest both for optical information processing [5,6] and for quantum communication [7] since optical photons are the ideal carriers of information over long distances. There are two main approaches to engineer the quantum state of an optical field [8]. First, by choosing the Hamiltonian correctly, one can utilize its time evolution to unitarily transform an initial state into the desired final state (e.g., generation of squeezed states and entangled photon pairs by parametric down-conversion). Second, by introducing entanglement between the system of interest and an auxiliary system followed by appropriate measurements on the auxiliary system, one can collapse the system of interest to the target state. This approach was used, for example, for the generation and entanglement of single photons in the DLCZ protocol for long-distance quantum communication [9], and in the recent generation of entangled atom–light Schrödinger cat states [10]. The two approaches may of course be combined, for instance, in the generation of optical Schrödinger cat states from squeezed vacuum, which is conditioned on the measurement of a subtracted photon diverted to an auxiliary mode [11]. QSE of

optical fields was discussed by Vogel *et al.* [12] in a paper proposing a recipe for generating an arbitrary quantum state in the field of a single-mode resonator. Following that, there have been considerable efforts on QSE of a traveling light field; from schemes preparing arbitrary quantum states using conditional measurements on beam splitters [13,14], to generating nonclassical states of specific interests, such as single-photon Fock states [15], Schrödinger cat states [11,16], NOON states [17], Greenberger–Horne–Zeilinger states [18,19], and cluster states [20]. Moreover, many different manipulations of the quantum field were realized, such as the annihilation and creation operators [21–23], squeezing [24], and quantum scissors [25].

At the heart of the study in this paper stands the single-photon Raman interaction (SPRINT) [26–28]. The configuration that leads to SPRINT was originally considered by Pinotsi and Imamoglu [29] as an ideal absorber of a single photon. It was later studied in a series of theoretical works [27,30–33] and shown to perform as a photon–atom swap gate and accordingly serve as a quantum memory. It was experimentally demonstrated with a single atom coupled to a whispering-gallery mode resonator and used to implement a single-photon router [34], extraction of a single photon from a pulse [26], and a photon–atom qubit swap gate [28]. In superconducting circuits it was demonstrated as well [35] and used for highly efficient detection of single microwave photons [36]. The SPRINT mechanism occurs in a three-level Λ system where

each transition is coupled to a single optical mode, as shown in Fig. 1 for the case of orthogonal polarizations H and V. As explained in detail in Ref. [27], in this configuration a single H (V) photon is enough to send the atom to the corresponding dark state $|g_v\rangle$ ($|g_h\rangle$). Symmetrically, the polarization of the returning photon is set by the initial state of the atom—which makes this configuration perform as a photon–atom swap gate [28]. In this work, we explore the potential of the SPRINT mechanism in multi-photon processes within the theoretical framework of the "modes of the universe" (MOU) [37,38]. Specifically, we show that a single SPRINT-based iteration involving an arbitrary input quantum state in one optical mode and a single-photon pulse in the other can realize the inverse of the annihilation operator [39], namely adds a single photon to the input state at success probability that scales inversely with the number of photons. Furthermore, repeating this process with the outgoing state for a number of iterations larger than the number of photons in the input pulse guarantees successful addition, which is heralded by a toggled state of a following readout photon. We then show that the success on n^{th} trial in fact implements what is best described as the nth-order bright quantum scissors (BQS) on the input state, which unlike regular quantum scissors (that truncate optical states to contain no more than one photon [25]) produce a state $|n+\rangle$ that contains at least n photons [Fig. 2(a)]. Beyond the fact that for certain input parameters these bright states approximate Fock states very well, we present a variation of the BQS scheme that ideally results in exact Fock states. Finally, we show that reversing the roles of the output channels and measuring the number of photons in the multi-photon output pulse collapses the train of single-photon pulses from the other output to a polarization W state [Fig. 2(b)].

The outline of this paper is organized as follows. In Section 2 we present the theoretical model in which our quantum state evolves. Section 3 is dedicated to presenting and acquiring intuition for SPRINT-based multi-photon processes. In Section 4 we introduce the multi-step protocol. Finally, in Section 5 we show how the inverse annihilation operator and the BQS can be employed on the traveling light field and how to produce the aforementioned Fock and W states.
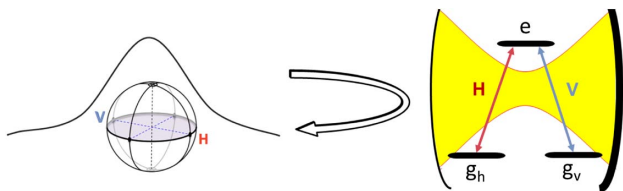
Fig. 1. Configuration that leads to single-photon Raman interaction (SPRINT). Two optical modes, in this case orthogonal polarizations (H and V), interacting with a three-level Λ system in a single-sided cavity. Each polarization is coupled to a different "leg" of the Λ system. Upon an incident H-polarized single-photon pulse and a Λ system prepared in $|g_h\rangle$, destructive interference forces the Λ system to emit back the photon in V and undergo a Raman transition to state $|g_v\rangle$. In effect this configuration realizes a unitary swap gate between the photonic and atomic qubit.
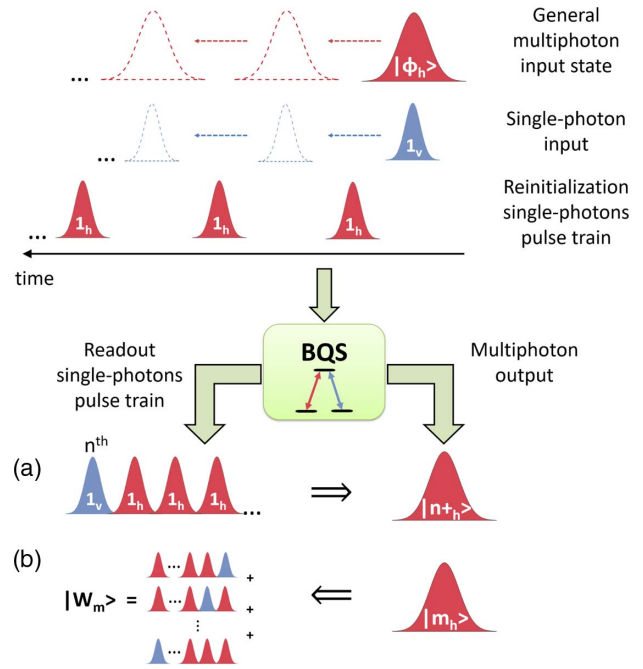
Fig. 2. Bright quantum scissors (BQS) multi-step protocol. The protocol uses three input channels: a general H-polarized multi-photon quantum state, a V-polarized single photon, and a train of H-polarized single photons. The multi-photon pulse and the V-polarized single-photon pulse interact with the Λ system simultaneously and the resulting pulses are fed back to the system repeatedly. The H-polarized single-photon pulses are interleaved with the multi-photon pulse evolutions and reinitialize the state of the Λ system at every iteration. At the output channels of the protocol we get a train of readout single-photon pulses and a modified multi-photon state. (a) Heralded on the measurement of the nth readout photon in the V-mode, the nth-order BQS operation is applied on the input quantum state. This ensures the presence of more than n photons in the multi-photon output. For $n = 1$, the operation amounts to a realization of the inverse annihilation. (b) Conversely, when choosing to herald on the number of photons in the multi-photon output pulse, a polarization W state manifests in the readout single-photons pulse train.

2. THEORETICAL FRAMEWORK

Consider the cavity-mediated interaction of an optical field with a three-level Λ system where each transition is coupled to one of two orthogonal polarizations; denote them as the horizontal (H) and vertical (V) polarizations (Fig. 1). Throughout this study we refer to the Λ system as an atom; however, this is merely a matter of convenience and should not limit the results to a specific physical implementation. Using the MOU approach, this system can be described by the following Hamiltonian [40]:

$$\mathcal{H} = -i\hbar g \int d\omega \frac{\sqrt{\kappa/\pi}}{\kappa - i\omega}(|e\rangle\langle g_h|\hat{a}_\omega + |e\rangle\langle g_v|\hat{b}_\omega)e^{-i(\omega+\delta)t} + \text{h.c.},$$

$$(1)$$

where κ is the cavity amplitude decay rate which is proportional to the width of its resonance. All the frequencies are relative to the cavity resonance frequency Ω_c; the detuning of the atomic transition from the resonance of the cavity is denoted by

$\delta = \Omega_c - \omega_a$ and the detuning of the actual light field frequency, Ω, from the cavity is denoted by $\omega = \Omega - \Omega_c$. The operators $\hat{a}_\omega$ and $\hat{b}_\omega$ are the annihilation operators for the H- and V-modes, respectively. These operators obey the continuum commutation relations in the frequency domain $[\hat{a}_\omega, \hat{a}_{\omega'}^\dagger] = [\hat{b}_\omega, \hat{b}_{\omega'}^\dagger] = \delta(\omega - \omega')$. The parameter g represents the cavity–atom coupling strength where $2g$ is the rate equal to the single-photon Rabi frequency.

Following Ref. [40], we work under several conditions. First, the cavity is on-resonance with the atomic transition, i.e., $\delta = 0$. Second, throughout the analytical derivation we assume that cavity losses and free-space spontaneous emission are negligible. Moreover, we assume two adiabatic limits related to T, the duration of the pulses we use; $\kappa T \gg 1$ and $\Gamma T \gg 1$ where $\Gamma = \frac{2g^2}{\kappa}$. In fact, Γ is the cavity-enhanced spontaneous emission rate of the atom to the mode of the cavity. Therefore, in these terms, the requirement of negligible free-space spontaneous emission translates to large cooperativity $C \equiv \frac{\Gamma}{\gamma} \gg 1$. Under these conditions our system is described effectively by Fig. 3, often referred to as the fast-cavity limit or the one-dimensional atom [41]. This space–time approach has been shown to be equivalent to the well-known "input–output" formalism [42–44] when the cavity transmission losses are small enough to allow for a Lorentzian approximation to the cavity resonance line [45].

It is necessary to introduce a few concepts that will help set the stage for developing the quantum state engineering protocol. As in Ref. [40], we will make use of the field annihilation operators

$$\hat{A}(t) \equiv \frac{1}{\sqrt{2\pi}} \int d\omega \hat{a}_\omega e^{-i\omega t}, \tag{2}$$

$$\hat{B}(t) \equiv \frac{1}{\sqrt{2\pi}} \int d\omega \hat{b}_\omega e^{-i\omega t}, \tag{3}$$

which can be thought of as the Fourier transform of the frequency domain operators $\hat{a}_\omega$ and $\hat{b}_\omega$. It is easy to see that these obey the continuum commutation relations in the time domain $[\hat{A}(t), \hat{A}^\dagger(t')] = [\hat{B}(t), \hat{B}^\dagger(t')] = \delta(t - t')$. In addition, we can define an N-photon wave packet in the H-mode in the following manner:

$$|N_h\rangle = \frac{1}{\sqrt{N!}} \left[\int dt f(t) \hat{A}^\dagger(t) \right]^N |0\rangle, \tag{4}$$

where $f(t)$ is the pulse shape of the wave packet and the state is normalized for $\int dt |f(t)|^2 = 1$. An N-photon wave packet in the V-mode, $|N_v\rangle$, can be described by simply replacing $\hat{A}^\dagger$ with $\hat{B}^\dagger$ in the expression above. Lastly, we introduce a state
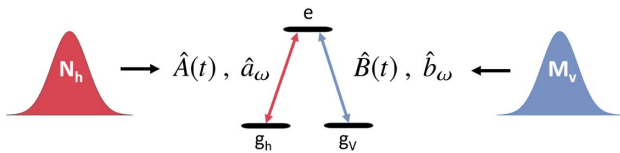
Fig. 3. One-dimensional atom. The effective system considered using the MOU approach in the adiabatic limit. Two modes of light, $\hat{a}_\omega$ and $\hat{b}_\omega$ [or $\hat{A}(t)$ and $\hat{B}(t)$], interact with the two transitions of an atom in a Λ configuration.

of N photons in the H-mode and a single photon in the V-mode; this state is time-entangled such that the V-photon is created in the kth time-slot (where $k \in \{1, \ldots, N + 1\}$):

$$|N_h, \overset{k^{\text{th}}}{1_v}\rangle \equiv \frac{\sqrt{(N+1)!}}{(k-1)!(N-k+1)!}$$

$$\times \int_{-\infty}^{\infty} dt \hat{B}^\dagger(t) f(t) \left[\int_{-\infty}^{t} dt_1 \hat{A}^\dagger(t_1) f(t_1) \right]^{k-1}$$

$$\times \left[\int_{t}^{\infty} dt_2 \hat{A}^\dagger(t_2) f(t_2) \right]^{N-k+1} |0\rangle. \tag{5}$$

In other words, as opposed to a the product state $|N_h\rangle \otimes |1_v\rangle$ where the time-ordering of the photons is unknown, in Eq. (5) we can be certain that the photon in the V-mode was created after exactly $(k - 1)$ photons in the H-mode. This time-entanglement is manifested in the integration limits of Eq. (5), in which the creation operator of a photon in the V-mode at time t is "sandwiched" between the creation of $(k - 1)$ photons in the H-mode before t, and $(N - k + 1)$ photons in the H-mode afterwards.

3. SPRINT-BASED TOOLBOX

SPRINT, previously presented in Refs. [27,46] using the input–output formalism, can be expressed in terms of the MOU approach. The evolution of initial state $|1_h, 0_v, g_h\rangle$ under Hamiltonian [Eq. (1)] is in fact a special case of the photon subtraction described in Ref. [40]; following the interaction with the atom, the initial state $|N_h, 0_v, g_h\rangle$ is transformed to the final state $|N - 1_h, \overset{1^{\text{st}}}{1_v}, g_v\rangle$. Substituting $N = 1$ in this result provides us with the desired effect, the initial H-photon is converted to a V-photon while the atom toggles from state $|g_h\rangle$ to $|g_v\rangle$:

$$|1_h, 0_v, g_h\rangle \rightarrow -|0_h, 1_v, g_v\rangle. \tag{6}$$

Utilizing SPRINT as a building block we can assemble a toolbox, which consists of the evolution of two specific states. The multi-step protocol in the next section leans heavily on these two processes - effective time-shifting and deterministic photon addition described in Eqs. (7a) and (7b), respectively:

$$|N_h, \overset{k^{\text{th}}}{1_v}, g_v\rangle \rightarrow |N_h, \overset{(k+1)^{\text{th}}}{1_v}, g_v\rangle, \tag{7a}$$

$$|N_h, \overset{(N+1)^{\text{th}}}{1_v}, g_v\rangle \rightarrow -|N + 1_h, 0_v, g_h\rangle. \tag{7b}$$

One can obtain these processes by solving the time-dependent Schrödinger equations associated with the evolution of the corresponding initial states in the same manner as in Ref. [40]. Instead of presenting the cumbersome derivation of these processes, we introduce a simple intuition for these results using SPRINT. Generally, we can picture a multi-photon process in the following way: in the adiabatic limit where the pulse is very long compared to the inverse of the cavity-enhanced decay rate, the probability of having two photons time-spaced by less than $\frac{1}{\Gamma}$ is negligible. Hence, we can conclude that each photon within the pulse interacts with the atom-cavity separately. When each photon reaches the atom-cavity, one in two may happen: if the atom is in the ground state matching the mode of the photon ($|1_v, g_v\rangle$ or $|1_h, g_h\rangle$), the resulting photon is emitted in the other mode and the atom toggles to the other ground state,

in accordance with SPRINT. In the other case, where the atom is in a ground state not matching the mode of the photon ($|1_h, g_v\rangle$ or $|1_v, g_h\rangle$), no interaction will occur since the optical field is not coupled to the relevant transition.

Now it is easy to get intuition for Eq. (7a). Since we start with the atom in $|g_v\rangle$, the first $(k-1)$ H-photons do not interact with the atom. The kth photon is in the V-mode; therefore, it experiences SPRINT, which results in the atom toggling to $|g_h\rangle$ and an H-photon emitted. Then for the $(k+1)^{\text{th}}$ H-photon we have SPRINT again (since the atom is now in $|g_h\rangle$), a V-photon is emitted leaving the atom in $|g_v\rangle$. The remaining $(N-k)$ H-photons in the pulse have no interaction with the atom. Consequently, the resulting state is a V-photon in the $(k+1)^{\text{th}}$ time-position and all the rest N photons in the H-mode. Overall, this process describes effective time-shifting of the V-photon, from the kth time-slot to the $(k+1)^{\text{th}}$ time-slot.

An exception to the above considerations is the case where $k = N+1$, i.e., the V-photon arrives last as noted in the initial state of Eq. (7b). Similarly, the first N H-photons do not interact with the atom and the $(N+1)^{\text{th}}$ V-photon experiences SPRINT, toggling the atom to $|g_h\rangle$ and emitting an H-photon. Since it was the last photon, we do not have another SPRINT as in the previous case. Therefore, we are left with $(N+1)$ H-photons and the atom in $|g_h\rangle$, which is the final state described in Eq. (7b). As a consequence, we get that the single photon in the V-photon is added deterministically to the N photons in the H-mode.

In general, we do not have time-entangled initial states at our disposal such as those used in the time-shifting and deterministic addition processes. Therefore, we present a mathematical identity [Eq. (8)] that links the product state $|N_h, 1_v\rangle$ to these time-entangled states. Basically, it describes this product state as an equal superposition of the time-entangled states representing all the different $(N+1)$ time-ordering of the photons. In essence, this summation over all the possible time-correlated states leads to a state where the arrival times of the V- and H-photons are completely uncorrelated:

$$|N_h, 1_v\rangle = \frac{1}{\sqrt{N+1}}\left(|N_h, \overset{1^{\text{st}}}{1_v}\rangle + \cdots + |N_h, \overset{(N+1)^{\text{th}}}{1_v}\rangle\right). \quad (8)$$

4. MULTI-STEP PROTOCOL

Based on Eqs. (6) and (7), we have constructed an iterative protocol for QSE. The first step of the protocol involves interacting the atom initialized in $|g_v\rangle$ with a multi-photon state comprised of two simultaneous pulses: a general H-polarized state and a single V-photon, $|\phi_h, 1_v\rangle$. Following the interaction, the pulses reflected off the cavity are rerouted back into the system by switchable mirrors (realized using Pockels cells) keeping the H- and V-modes the same (Fig. 4). While these pulses are being rerouted, we send an additional single H-photon in order to reinitialize the atom to $|g_v\rangle$ using SPRINT [Eq. (6)]. As a result, either an H- or a V-photon can be emitted, depending on the final state of the atom after the initial pulses have completed the interaction. Subsequently, the rerouted multi-photon state interacts with the atom once again. This sequence is repeated as depicted in Fig. 5; we refer to a single iteration of the protocol as interacting the multi-photon state (or its evolutions) with the
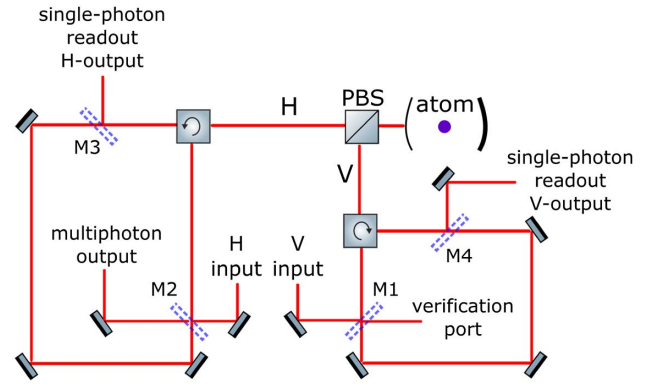
Fig. 4. Optical setup suitable for the implementation of the BQS protocol. H-input and V-input are the sources for the pulses in the two modes. Switchable mirrors M1–M4 are used to repeatedly alternate between directing the readout photons to their respective outputs and rerouting the multi-photon state back into the cavity. Upon measuring a photon in the "single-photon readout V-output" on the nth iteration of the protocol, M2 is turned ON and an $|n+\rangle$ state is measured in "multi-photon output." On the other hand, when heralding on vacuum in the verification port and M photons in the multi-photon output, a W state is generated at the combination of single-photon readout H- and V-output.
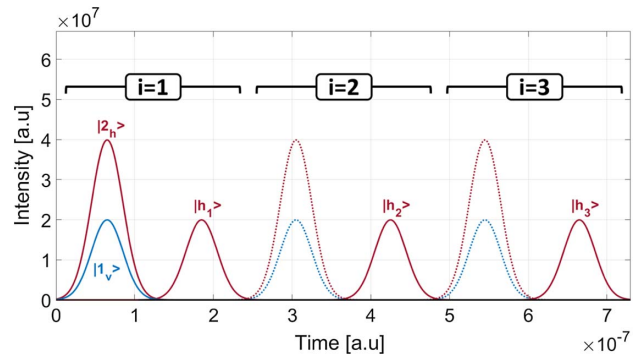
Fig. 5. Pulse sequence for $|\phi_h\rangle = |2_h\rangle$. The H- and V-modes are represented by red and blue, respectively. Solid lines refer to pulses we send actively from H- and V-input while dotted lines represent those redirected back into the cavity. The iteration number appears above the relevant pulses.

atom followed by reinitializing the atom. The train of single photons resulting from the reinitialization photons is henceforth referred to as "readout photons" and denoted as $|h_i\rangle$ or $|v_i\rangle$ where the subscript indicates the number of iteration. The readout photons are directed to the single-photon readout output (either H or V) by switchable mirrors (M3 and M4), and thus separated from the multi-photon state. Finally, upon proper heralding on the readout channel we can realize the inverse annihilation and bright scissors operation on the multi-photon state. On the other hand, heralding on the multi-photon output channel and the verification port (using M1 and M2), we can generate polarization W states in the readout photons. These are discussed in detail in Section 5.

In order to get intuition for the iterative protocol we examine the evolution of the initial state $|1_h, 1_v, g_v\rangle$ in Eq. (9).

For convenience, we denote the interaction of the multi-photon state with the atom as $\overset{\text{atom}}{\rightarrow}$ and the jth reinitialization of the atom using an H-photon by $\overset{h_j}{\rightarrow}$. Using Eq. (8) and the tools provided in Eqs. (6) and (7) it is simple to follow the evolution of the state throughout the protocol:

$$|1_h, 1_v, g_v\rangle = \frac{1}{\sqrt{2}}(|1_h, \overset{\text{2nd}}{1_v}\rangle + |1_h, \overset{\text{1st}}{1_v}\rangle) \otimes |g_v\rangle$$

$$\overset{\text{atom}}{\rightarrow} \frac{1}{\sqrt{2}}(-|2_h, 0_v, g_h\rangle + |1_h, \overset{\text{2nd}}{1_v}, g_v\rangle)$$

$$\overset{h_1}{\rightarrow} \frac{1}{\sqrt{2}}(|2_h, 0_v, g_v\rangle \otimes |v_1\rangle + |1_h, \overset{\text{2nd}}{1_v}, g_v\rangle \otimes |h_1\rangle)$$

$$\overset{\text{atom}}{\rightarrow} \frac{1}{\sqrt{2}}(|2_h, 0_v, g_v\rangle \otimes |v_1\rangle - |2_h, 0_v, g_h\rangle \otimes |h_1\rangle)$$

$$\overset{h_2}{\rightarrow} \frac{1}{\sqrt{2}}|2_h, 0_v, g_v\rangle \otimes (|v_1, h_2\rangle + |h_1, v_2\rangle)$$

$$\rightarrow \underbrace{\cdots}_{2 \leq k+1 \text{ iterations}} \rightarrow |2_h, 0_v, g_v\rangle$$

$$\otimes \frac{1}{\sqrt{2}}(|v_1, h_2, h_3, \ldots, h_{k+1}\rangle + |h_1, v_2, h_3, \ldots, h_{k+1}\rangle). \quad (9)$$

It is constructive to think of the protocol in terms of photon addition. The state $|N_h, 1_v\rangle$ has an equal probability of having each of the $(N + 1)$ possible time-orderings of the V-photon [Eq. (8)]. For the time-ordering in which the V-photon is last, the resulting field state after interaction with the atom is $|N + 1_h, 0_v\rangle$ [Eq. (7a)], i.e., the V-photon was added to the H-mode. As for the other possible time-orderings, the time-position of the V-photon will move one slot to a later time [Eq. (7b)]. Therefore, $(N + 1)$ repeated attempts of photon addition with the initial $|N_h, 1_v\rangle$ state guarantee that the V-photon is added to the H-mode. In our iterative scheme, the additional H-photon we send serves two goals. First, it re-initializes the atom to $|g_v\rangle$ allowing repeated addition attempts. Second, since a successful addition leaves the atom in $|g_h\rangle$, the following emitted readout photon tells us whether the addition was successful (V-photon) or not (H-photon). Hence, through entanglement of our state to the readout photons, we have information about when (at which iteration or attempt) did a successful addition occur. With this in mind, we can generalize Eq. (9) to an initial $|N_h, 1_v\rangle$ state and look at the outcome of the protocol after $(k + 1)$ iterations:

We can now determine the outcome of any initial state in the H-mode and a single photon in the V-mode. Expanding the arbitrary state in the H-mode using the Fock basis we can write the initial state as

$$|\psi_{\text{initial}}\rangle = |\phi_h, 1_v\rangle = \sum_{N=0}^{\infty} C_N |N_h, 1_v\rangle. \quad (11)$$

Using Eq. (10) we can get the resulting state after $(k + 1)$ iterations of the scheme:

$$|\psi_{\text{final}}\rangle$$
$$= |v_1, h_2, h_3, \ldots, h_{k+1}\rangle \otimes \left(\sum_{N=0}^{\infty} \frac{C_N}{\sqrt{N+1}} |N + 1_h\rangle \right) |0_v, g_v\rangle$$

$$+ |h_1, v_2, h_3, \ldots, h_{k+1}\rangle \otimes \left(\sum_{N=1}^{\infty} \frac{C_N}{\sqrt{N+1}} |N + 1_h\rangle \right) |0_v, g_v\rangle$$

$$+ \cdots$$

$$+ |h_1, \ldots, h_k, v_{k+1}\rangle \otimes \left(\sum_{N=k}^{\infty} \frac{C_N}{\sqrt{N+1}} |N + 1_h\rangle \right) |0_v, g_v\rangle$$

$$+ |h_1, \ldots, h_{k+1}\rangle \otimes \sum_{N=k+1}^{\infty} \frac{C_N}{\sqrt{N+1}} (|N_h, \overset{(k+2)^{\text{th}}}{1_v}\rangle$$

$$+ \cdots + |N_h, \overset{(N+1)^{\text{th}}}{1_v}\rangle) |g_v\rangle. \quad (12)$$

Heralding differently will allow us to engineer quantum states and implement various operations.

5. RESULTS

A. Inverse Annihilation

Since the annihilation operator has an eigenvalue of zero for $\hat{a}|0\rangle = 0$, we cannot find an operator $\hat{O}$ such that $\hat{O}\hat{a} = I$. On the other hand, we can find $\hat{O}$, which satisfies $\hat{a}\hat{O} = I$; this is known as the inverse annihilation operator $\hat{a}^{-1}$ [39],

$$\hat{a}\hat{a}^{-1} = I; \qquad \hat{a}^{-1}\hat{a} = I - |0\rangle\langle 0|. \quad (13)$$

In the Fock basis representation it has the form

$$\hat{a}^{-1} = \sum_{n=0}^{\infty} \frac{1}{\sqrt{n+1}} |n + 1\rangle\langle n|. \quad (14)$$

It is important to make the distinction between this operator and the creation operator,

$$|N_h, 1_v, g_v\rangle \overset{k+1}{\underset{\text{iterations}}{\rightarrow}} \begin{cases} \text{for } k \geq N: \\ |N + 1_h, 0_v, g_v\rangle \otimes \frac{1}{\sqrt{N+1}}(|v_1, h_2, h_3, \ldots, h_{k+1}\rangle + |h_1, v_2, h_3, \ldots, h_{k+1}\rangle \\ + \cdots + |h_1, \ldots, h_N, v_{N+1}, h_{N+2}, \ldots, h_{k+1}\rangle) \\ \text{for } k \leq N - 1: \\ |N + 1_h, 0_v, g_v\rangle \otimes \frac{1}{\sqrt{N+1}}(|v_1, h_2, h_3, \ldots, h_{k+1}\rangle + |h_1, v_2, h_3, \ldots, h_{k+1}\rangle \cdot \\ + \cdots + |h_1, \ldots, h_k, v_{k+1}\rangle) \\ + \frac{1}{\sqrt{N+1}} \underbrace{(|N_h, \overset{(k+2)^{\text{th}}}{1_v}, g_v\rangle + \cdots + |N_h, \overset{(N+1)^{\text{th}}}{1_v}, g_v\rangle)}_{(N-k) \text{ terms}} \otimes |h_1, \ldots, h_{k+1}\rangle \end{cases} \quad (10)$$

$$\hat{a}^\dagger = \sum_{n=0}^{\infty} \sqrt{n+1}\,|n+1\rangle\langle n|, \tag{15}$$

which is simply the Hermitian conjugate of $\hat{a}$. As evident, besides adding a photon, the two operators affect the target state by changing the coefficients of Fock-state components. Intuitively speaking, this change reflects the knowledge gained on the state by the fact that the photon was successfully added. This results in higher likelihood of large Fock states in the case of the creation operator (reflecting the Bosonic amplification), and lower likelihood of large Fock states in the case of the inverse annihilation operator. In this sense, both operators differ from the addition operator,

$$\hat{S}^+ = \sum_{n=0}^{\infty} |n+1\rangle\langle n|, \tag{16}$$

which does not alter the target state in any way except adding one photon as was demonstrated with phonons of a trapped ion system [47].

The operation of the inverse annihilation can be achieved using only a single step of the protocol presented above. Looking at Eq. (12) we can see that if we herald on $|v_1\rangle$, this is exactly the operation we get for the initial H-mode state $|\phi_h\rangle = \sum_{N=0}^{\infty} C_N |N_h\rangle$. Since we herald on $|v_1\rangle$ we need just one iteration of the protocol, i.e., $k=0$:

$$\langle v_1 | \psi_{\text{final}} \rangle = \left(\sum_{N=0}^{\infty} \frac{C_N}{\sqrt{N+1}} |N+1_h\rangle \right) |0_v, g_v\rangle$$

$$\overset{\star}{\to} \sum_{N=0}^{\infty} \frac{C_N}{\sqrt{N+1}} |N+1_h\rangle$$

$$= \hat{a}^{-1} \sum_{N=0}^{\infty} C_N |N_h\rangle = \hat{a}^{-1} |\phi_h\rangle, \tag{17}$$

where in $\star$ we trace over the atom and the V-mode. This effect is actually described in Ref. [40] as a probabilistic photon addition but in fact, since it changes the photon number statistics, it does not function as the addition operator [Eq. (16)] but rather as the inverse annihilation [Eq. (14)].

Fidelity and efficiency are used to characterize the quality of a process. Fidelity is a measure to quantify accuracy, and it is the overlap between the final state of the process and the ideal, desired state. Efficiency, on the other hand, is the probability to obtain this final state by the end of the process. Upon heralding on $|v_1\rangle$, the process is of unit fidelity and the efficiency of this process is given by

$$\eta_1 = \sum_{N=0}^{\infty} \frac{|C_N|^2}{N+1}. \tag{18}$$

For an initial coherent state $|\alpha\rangle$ in the H-mode we get the efficiency of the inverse annihilation operator presented in Fig. 6.

B. Bright Quantum Scissors

One may characterize a quantum state $|\psi\rangle$ using its photon-number distribution defined by the probabilities $P(N) = |\langle N|\psi\rangle|^2$. The kth-order BQS operation truncates any input quantum state such that the modified state has at least k photons, i.e., $P(N < k) = 0$. This is in some sense complementary to the well-known quantum scissors introduced in
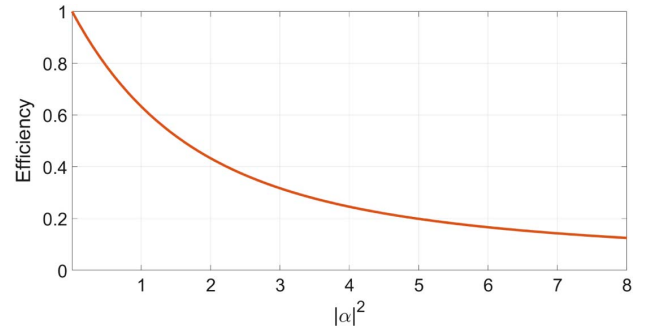
Fig. 6. Efficiency of $\hat{a}^{-1}$ as a function of $|\alpha|^2$, the average number of photons in the initial coherent state.

Ref. [25], which leaves only the vacuum and one-photon components of the quantum state. Looking at Eq. (12), we see that heralding on $|v_k\rangle$ ensures the operation of the kth-order BQS:

$$\langle v_k | \psi_{\text{final}} \rangle = \underbrace{|h_1, h_2, \ldots, h_{k+1}\rangle}_{\text{trace out}}$$

$$\otimes \left(\sum_{N=k-1}^{\infty} \frac{C_N}{\sqrt{N+1}} |N+1_h\rangle \right) \otimes \underbrace{|0_v, g_v\rangle}_{\text{trace out}}$$

$$\to \mathcal{N} \sum_{N=k}^{\infty} \frac{C_{N-1}}{\sqrt{N}} |N_h\rangle \equiv |k+\rangle, \tag{19}$$

where $\mathcal{N}$ is a normalization factor. This resulting state is highly non-classical since the probability $P(N < k)$ vanishes [48]. The process is of unit fidelity and the efficiency of the kth-order BQS is given by

$$\eta_2 = \sum_{N=k}^{\infty} \frac{|C_{N-1}|^2}{N}. \tag{20}$$

For an input coherent state in the H-mode we get the efficiency presented in Fig. 7.

As previously discussed, for an initial $|N_h, 1_v\rangle$, addition is guaranteed after $(k+1)$ or more iterations and the resulting readout V-photon tells us at which iteration did it occur. Therefore, by choosing the number of iterations such that $P(N \geq k+1)$ of the general input state is negligible [Eq. (21)], we can be certain that addition occurred for all of its number state components. In this way, the overall
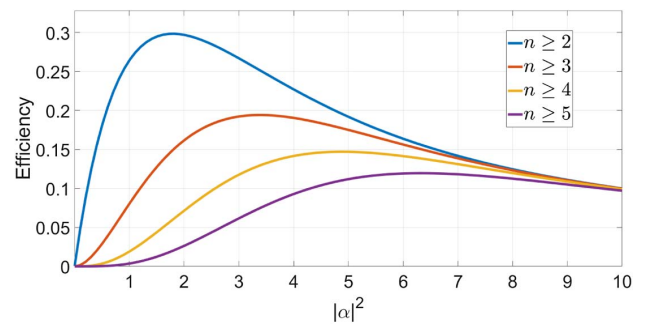
Fig. 7. n^{th}-order BQS. Efficiency as a function of the average number of photons in the initial coherent state, $|\alpha|^2$. The resulting state $|n+\rangle$ is guaranteed to have more than n photons.

BQS operation (including its 1st-order interpretation as the inverse annihilation) can be made to succeed deterministically. The success of any specific order of the BQS is then heralded by detection of the V-photon at the desired iteration:

$$P(N \geq k+1) = \sum_{N=k+1}^{\infty} |C_N|^2 \ll 1. \qquad (21)$$

As can be seen from Eq. (12), the probability of BQS acting on the input state after $(k+1)$ iterations is given by

$$\eta_{BQS} = 1 - \sum_{N=k+1}^{\infty} \frac{(N-k)|C_N|^2}{N+1}. \qquad (22)$$

In the case where the number of iterations and the photon-number distribution of the input state maintain Eq. (21), the sum in Eq. (22) vanishes, guaranteeing the success of the BQS operation.

BQS can also be used to generate Fock states from coherent state input (Fig. 8) by choosing $|\alpha|^2$ small enough such that the probability of $|k\rangle$ in the resulting state [Eq. (19)] will be much larger than that of $|k+1\rangle$ and higher components. The relation between these probabilities will determine the fidelity of the Fock state. Clearly, there is a trade-off between the efficiency and the fidelity of the process; choosing a lower average number of photons in the coherent state results in higher fidelity since the probabilities of $|k+1\rangle$ or higher components decrease relative to the probability of $|k\rangle$. On the other hand, this low number of photons also leads to a low efficiency. A better scheme for producing Fock states is described in Subsection 5.C.

The BQS described in Eq. (19) alters the ratio between the amplitudes of the remaining number states. If we wish to "cut the tail" of the photon-number distribution while also keeping the ratios of the initial state [Eq. (11)] the same, we can operate on our initial state with the BQS followed by the annihilation operator (typically using a high-transmittivity beam splitter [21]). This results in

$$\hat{a} \mathcal{N} \sum_{N=k}^{\infty} \frac{C_N}{\sqrt{N+1}} |N+1_h\rangle = \mathcal{N} \sum_{N=k}^{\infty} C_N |N_h\rangle, \qquad (23)$$

which is equivalent to the operator

$$\hat{O} = \hat{I} - \sum_{n=0}^{k-1} |n\rangle\langle n| \qquad (24)$$
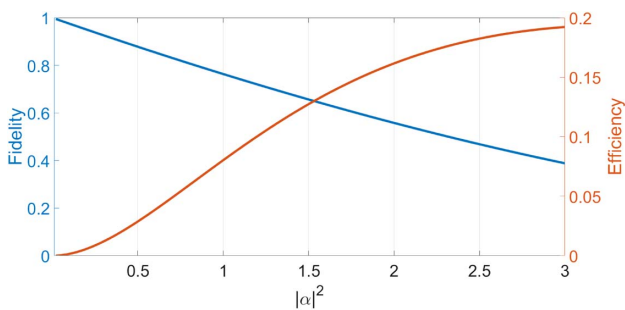
Fig. 8. Generation of a Fock state $|3\rangle$ using the 3rd-order BQS. Fidelity and efficiency as functions of the average number of photons in the coherent state.

acting on the H-polarized initial state. Hence, at the price of an additional iteration and a decrease in efficiency due to the annihilation process, we can get a neutral-BQS operation that maintains the ratio between probability amplitudes of the initial state.

C. Fock State Generation

Using an interference-based measurement of two consecutive readout photons, we are able to generate Fock states with unit fidelity. For this purpose, we must alter the readout output ports in order to realize a Bell state measurement (Fig. 9).

Consider an entangled state in the form

$$|\chi\rangle = |v_k\rangle|h_{k+1}\rangle|\psi_1\rangle + |h_k\rangle|v_{k+1}\rangle|\psi_2\rangle. \qquad (25)$$

After passing through the optical setup we have four possible modes for the two readout photons reaching the 50:50 beam splitter simultaneously; two different incoming ports denoted by the subscript and two different polarizations, vertical (V) and horizontal (H). Therefore, we can rewrite the state as

$$|\chi\rangle = |V_1 H_2\rangle|\psi_1\rangle + |H_1 V_2\rangle|\psi_2\rangle. \qquad (26)$$

Then, heralding on coincident detections in the two photodetectors we collapse on the antisymmetric Bell state [49]

$$\pm \frac{1}{\sqrt{2}} \langle \psi^{(-)}| = \pm \frac{1}{\sqrt{2}} (\langle V_1 H_2| - \langle H_1 V_2|). \qquad (27)$$
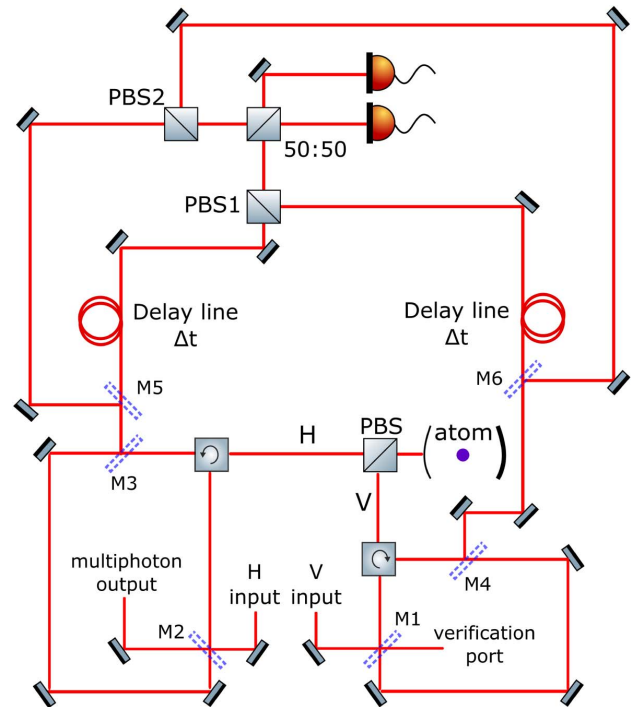
Fig. 9. Optical setup for Fock state generation via Bell state measurement. First, we direct the kth readout photon (either H or V) to a delay line (mirrors M5 and M6 are OFF). When the $(k+1)$th readout photon leaves the cavity, we turn M5 and M6 ON in order to direct it to the path with no time delay. The delay time is set such that both the kth and the $(k+1)$th readout photons enter the 50:50 beam splitter simultaneously. Coincident detections at the output of the 50:50 beam splitter guarantee that our state has collapsed on the antisymmetric Bell state [49].

Therefore,

$$\pm \frac{1}{\sqrt{2}} \langle \psi^{(-)}| \chi \rangle = \pm \frac{1}{\sqrt{2}} (|\psi_1\rangle - |\psi_2\rangle). \tag{28}$$

Implementing this measurement on our final state in Eq. (12) for the kth and the $(k+1)^{\text{th}}$ outgoing readout photons we get (ignoring the overall sign)

$$\frac{1}{\sqrt{2}} (\langle v_k, h_{k+1}| - \langle h_k, v_{k+1}|)|\psi_{\text{final}}\rangle$$

$$= \frac{1}{\sqrt{2}} \underbrace{|h_1, ..., h_{k-1}\rangle \otimes |0_v, g_v\rangle}_{\text{trace out}}$$

$$\otimes \left(\sum_{N=k-1}^{\infty} \frac{C_N}{\sqrt{N+1}} |N+1_h\rangle - \sum_{N=k}^{\infty} \frac{C_N}{\sqrt{N+1}} |N+1_h\rangle \right)$$

$$= \frac{1}{\sqrt{2}} \frac{C_{k-1}}{\sqrt{k}} |k_h\rangle. \tag{29}$$

This means that heralding on coincident detections of the kth and $(k+1)^{\text{th}}$ readout photons we get a Fock state of $|k\rangle$ with unit fidelity and an efficiency given by

$$\eta_3 = \frac{|C_{k-1}|^2}{2k}. \tag{30}$$

We can understand it intuitively as interfering two BQS operations; one providing an output state containing more than k photons and the other a state with more than $(k+1)$ photons. Then, if the interference is with a minus sign, we get a telescoping sum leaving just the Fock state of $|k\rangle$.

Using an input coherent state $|\alpha\rangle$ we can optimize the efficiency of generating Fock state $|k\rangle$ by choosing the average number of photons $|\alpha|^2 = k-1$ such that $|C_{k-1}|^2$ is maximized. The efficiency in that case is given by

$$\eta_4 = \frac{1}{2k!} \left(\frac{k-1}{e} \right)^{k-1}. \tag{31}$$

Figure 10 presents this optimal efficiency for generating various Fock states. This efficiency scales like $\frac{1}{\sqrt{k}}$ compared to the maximal heralding probability of generating Fock states from optimally squeezed states, as calculated from fundamental principles [50].

D. W State Generation
An n-qubit W state in the polarization basis is defined for $n \geq 3$ below:
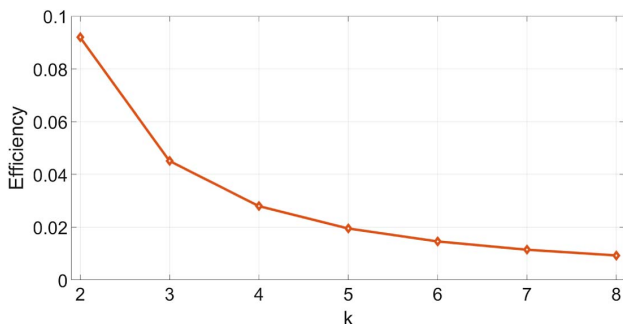
Fig. 10. Efficiency of generating a Fock state $|k\rangle$ by using an optimal coherent state input (see text).

$$|W_n\rangle = \frac{1}{\sqrt{n}} (|VHH...H\rangle + |HVH...H\rangle + \cdots$$

$$+ |HH...HV\rangle). \tag{32}$$

In order to generate W states using the BQS protocol we reverse roles; heralding is performed on the multi-photon output and the resulting W state is comprised of the readout photons. It is then constructive to rearrange the terms in the final state of the protocol [Eq. (12)] to the following form:

$$|\psi_{\text{final}}\rangle$$

$$= \sum_{N=0}^{k-1} \frac{C_N}{\sqrt{N+1}} |N+1_h, 0_v, g_v\rangle \otimes (|v_1, h_2, h_3, ..., h_{k+1}\rangle$$

$$+ |h_1, v_2, h_3, ..., h_{k+1}\rangle + \cdots$$

$$+ |h_1, ..., h_N, v_{N+1}, h_{N+2}, ..., h_{k+1}\rangle)$$

$$+ \sum_{N=k}^{\infty} \frac{C_N}{\sqrt{N+1}} |N+1_h, 0_v, g_v\rangle \otimes (|v_1, h_2, h_3, ..., h_{k+1}\rangle$$

$$+ |h_1, v_2, h_3, ..., h_{k+1}\rangle + \cdots + |h_1, ..., h_k, v_{k+1}\rangle)$$

$$+ \sum_{N=k+1}^{\infty} \frac{C_N}{\sqrt{N+1}} \left(|N_h, \overset{(k+2)^{\text{th}}}{1_v}, g_v\rangle + \cdots \right.$$

$$\left. + |N_h, \overset{(N+1)^{\text{th}}}{1_v}, g_v\rangle \right) \otimes |h_1, ..., h_{k+1}\rangle. \tag{33}$$

Following the operation of the protocol for three or more iterations, we deflect the multi-photon state to the multi-photon output and verification port using mirrors M1 and M2 (see Fig. 4). If one measures the multi-photon output in the state of $|M_h, 0_v\rangle$ (for $M \geq 3$), then the remaining readout photons collapse to

$$\langle M_h, 0_v|\psi_{\text{final}}\rangle$$

$$= \frac{C_{M-1}}{\sqrt{M}} |g_v\rangle \otimes \begin{cases} \textbf{for } 3 \leq M \leq k: \\ |v_1, h_2, h_3, ..., h_{k+1}\rangle + |h_1, v_2, h_3, ..., h_{k+1}\rangle \\ + \cdots + |h_1, ..., h_{M-1}, v_M, h_{M+1}, ..., h_{k+1}\rangle \\ \textbf{for } M \geq k+1: \\ |v_1, h_2, h_3, ..., h_{k+1}\rangle + |h_1, v_2, h_3, ..., h_{k+1}\rangle \\ + \cdots + |h_1, ..., h_k, v_{k+1}\rangle \end{cases}. \tag{34}$$

Tracing over the state of the atom, renormalizing and using Eq. (32) results in

$$\langle M_h, 0_v|\psi_{\text{final}}\rangle$$

$$= \begin{cases} |W_M\rangle \otimes |h_{M+1}, ..., h_{k+1}\rangle & \text{for } 3 \leq M \leq k \\ |W_{k+1}\rangle & \text{for } M \geq k+1 \end{cases}. \tag{35}$$

We can think of the generation of W states in the following manner: whenever we find vacuum in the verification port and $M \geq 3$ H-photons in the multi-photon output, we are guaranteed to have a unit-fidelity W state manifested in the time-separated readout photons. In the case where M is greater than or equal to the number of iterations we get a W state with the number of qubits equal to the number of iterations. On the
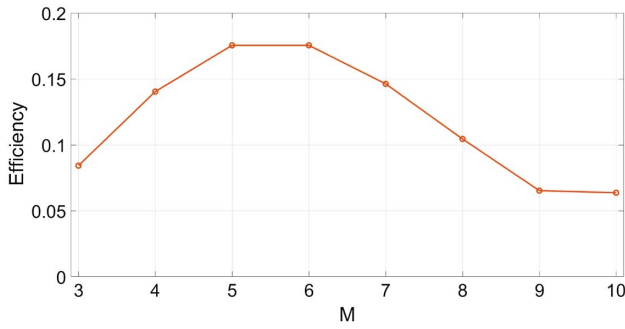
Fig. 11. Efficiency for generating W_M states by using an initial coherent state with average photon number of 5 and applying the protocol for 10 iterations.

other hand, when M is smaller than the number of iterations, we get a W state of size M and additional $(k - M)$ H-photons that may be ignored for any practical purpose.

As an example, examine the action of 10 iterations of the protocol on an initial coherent state with average photon number of five in the H-mode. The success probability for generating a $|W_M\rangle$ state is depicted in Fig. 11. Notice that the sum of these probabilities approaches unity ($\sim96\%$); therefore, we are almost guaranteed to find a W state by the end of the protocol. This is always the case when the number of iterations of the protocol is larger than the number of photons in the multiphoton input state, as in the BQS operation (see Section 5.B). In addition, since the success probability of $|W_{k+1}\rangle$ is comprised of all the contributions of more than $(k + 1)$ signal photons in the H-mode, there is a clear enhancement of the success probability for $|W_{10}\rangle$.

6. FEASIBILITY

There are a few issues that need addressing in terms of experimental feasibility. The scheme assumes an on-demand single-photon source for the initial V-mode and for the train of H-photons, as well as unit single-photon detection probability for indication and heralding. It also assumes high cooperativity, namely negligible interaction with optical modes that are not Purcell-enhanced by the cavity. In all these, significant progress has been made in recent years. The field of all-optical quantum information processing has motivated major efforts both toward the attainment of deterministic single-photon sources, quantum-dot-based [51–53] and others [54,55], and toward efficient superconducting single-photon detectors [56]. Novel waveguide and cavity technology, photonic bandgap in particular, reach cooperativities approaching 10^2 [57]. However, the most deleterious issue is optical loss. In order to get intuition on the effects of loss on the fidelity of this scheme, consider the production of a Fock state of $|3\rangle$ using the bright scissors operation (Fig. 8) with an initial H-mode coherent pulse of $\langle N \rangle = 0.02$. Upon correct heralding, i.e., measuring $|h_1, h_2, v_3\rangle$, it is most probable that the outgoing state has evolved from the initial $|2_h, \overset{\text{1st}}{1}_v\rangle$ component of the coherent state. This is so since a lower number of photons cannot result in a $|v_3\rangle$ photon (successful addition in the third attempt), while the higher number of photons is less probable by several

orders of magnitude due to the low average number of photons. In addition, any other time-ordering of the $|2_h, 1_v\rangle$ state where the V-photon is not first, will not lead to a $|v_3\rangle$ photon. Then let us examine the evolution of $|2_h, \overset{\text{1st}}{1}_v\rangle$ through the three repetitions of the protocol; a loss of a photon or more during the first repetition will result in one of the following: $|2_h, 0_v\rangle$, $|1_h, \overset{\text{2nd}}{1}_v\rangle$, $|1_h, 0_v\rangle$, $|0_h, 1_v\rangle$, and $|0\rangle$. None of those states can result in $|h_1, h_2, v_3\rangle$ since they will either toggle the atom on the next step producing $|v_2\rangle$ or not toggle the atom at all leading to no readout V-photon during the entire protocol. Hence, the loss on the first repetition will not affect the fidelity and we can consider the ideal state $|2_h, \overset{\text{2nd}}{1}_v\rangle$ as the only one contributing to the next steps. In contrast, during the second and third repetitions, a loss of a photon could still generate the correct heralding but the protocol will not result in the final Fock state $|3\rangle$. Hence, the fidelity is governed by a factor of $(1 - L)^6$ (where L is the loss of the cavity) signifying that no photon was lost in any of the six SPRINT interactions of these two repetitions. This power law, which appears for other cases as well, amounts to a significant decrease in fidelity and poses an obstacle for the experimental implementation of such a multi-step protocol. Nonetheless, the ongoing technological development in manufacturing high-Q and low-loss optical resonators [58–60], is expected to bring the demonstration of W and Fock states with moderate number of photons to within reach in the near future.

7. SUMMARY

In this work we described a protocol for optical QSE that performs the BQS operation on any input quantum state. The protocol is based on repeated SPRINT iterations of the input state together with single-photon pulses, carried out by a single Λ system in a single-sided cavity in the Purcell regime. We note that strong coupling is not necessary for SPRINT, as well as for most photon–atom gates [61]. The special case of a single iteration of the BQS protocol realizes the inverse annihilation operator. Multiple iterations can be used to deterministically generate a single pulse in a bright quantum state $|n+\rangle$ that has at least n photons, or a train of single photon pulses in a $|W_n\rangle$ state. In both cases the specific value of n is indicated by a measurement at the other output port, and the probabilities for different values of n are determined by the initial input quantum state (e.g., a coherent state $|\alpha\rangle$). While at certain input parameters the state $|n+\rangle$ approximates well the Fock state $|n\rangle$, a variation of the protocol can be used to produce heralded exact Fock states. The main vulnerability of the protocol is linear loss, which hampers its scaling-up to a large number of photons. Accordingly, our efforts are now aimed at adding more heralding mechanisms into the protocol, to allow maintaining fidelity of the generated states at the expense of lower efficiency. Nonetheless, with the advancements of technologies for efficient generation and detection of single photons, together with the ongoing efforts toward coupling quantum emitters such as atoms, ions, quantum dots, and spin-systems to low-loss, high-quality waveguides and resonators [58–60,62,63], this protocol could serve as a versatile building-block for QSE in quantum

communication, distributed quantum information processing, and all-optical quantum computing.

REFERENCES

1. J.-W. Pan, D. Bouwmeester, M. Daniell, H. Weinfurter, and A. Zeilinger, "Experimental test of quantum nonlocality in three-photon Greenberger-Horne–Zeilinger entanglement," Nature **403**, 515–519 (2000).
2. C. H. Bennett, G. Brassard, C. Crépeau, R. Jozsa, A. Peres, and W. K. Wootters, "Teleporting an unknown quantum state via dual classical and Einstein-Podolsky-Rosen channels," Phys. Rev. Lett. **70**, 1895–1899 (1993).
3. H. Jeong, M. S. Kim, and J. Lee, "Quantum-information processing for a coherent superposition state via a mixed entangled coherent channel," Phys. Rev. A **64**, 052308 (2001).
4. LIGO-collaboration, "A gravitational wave observatory operating beyond the quantum shot-noise limit," Nat. Phys. **7**, 962–965 (2011).
5. E. Knill, R. Laflamme, and G. J. Milburn, "A scheme for efficient quantum computation with linear optics," Nature **409**, 46–52 (2001).
6. P. Walther, K. J. Resch, T. Rudolph, E. Schenck, H. Weinfurter, V. Vedral, M. Aspelmeyer, and A. Zeilinger, "Experimental one-way quantum computing," Nature **434**, 169–176 (2005).
7. K. Azuma, K. Tamaki, and H.-K. Lo, "All-photonic quantum repeaters," Nat. Commun. **6**, 6787 (2015).
8. F. Dell'Anno, S. De Siena, and F. Illuminati, "Multiphoton quantum optics and quantum state engineering," Phys. Rep. **428**, 53–168 (2006).
9. L.-M. Duan, M. Lukin, J. I. Cirac, and P. Zoller, "Long-distance quantum communication with atomic ensembles and linear optics," Nature **414**, 413–418 (2001).
10. B. Hacker, S. Welte, S. Daiss, A. Shaukat, S. Ritter, L. Li, and G. Rempe, "Deterministic creation of entangled atom–light Schrödinger-cat states," Nat. Photonics **13**, 110–115 (2019).
11. A. Ourjoumtsev, R. Tualle-Brouri, J. Laurat, and P. Grangier, "Generating optical Schrodinger kittens for quantum information processing," Science **312**, 83–86 (2006).
12. K. Vogel, V. Akulin, and W. Schleich, "Quantum state engineering of the radiation field," Phys. Rev. Lett. **71**, 1816–1819 (1993).
13. M. Dakna, J. Clausen, L. Knöll, and D.-G. Welsch, "Generation of arbitrary quantum states of traveling fields," Phys. Rev. A **59**, 1658–1661 (1999).
14. J. Fiurášek, R. García-Patrón, and N. J. Cerf, "Conditional generation of arbitrary single-mode quantum states of light by repeated photon subtractions," Phys. Rev. A **72**, 033822 (2005).
15. A. I. Lvovsky, H. Hansen, T. Aichele, O. Benson, J. Mlynek, and S. Schiller, "Quantum state reconstruction of the single-photon Fock state," Phys. Rev. Lett. **87**, 050402 (2001).
16. A. Ourjoumtsev, H. Jeong, R. Tualle-Brouri, and P. Grangier, "Generation of optical Schrodinger cats from photon number states," Nature **448**, 784–786 (2007).
17. I. Afek, O. Ambar, and Y. Silberberg, "High-noon states by mixing quantum and classical light," Science **328**, 879–881 (2010).
18. D. Bouwmeester, J.-W. Pan, M. Daniell, H. Weinfurter, and A. Zeilinger, "Observation of three-photon Greenberger-Horne-Zeilinger entanglement," Phys. Rev. Lett. **82**, 1345–1349 (1999).
19. D. R. Hamel, L. K. Shalm, H. Hübel, A. J. Miller, F. Marsili, V. B. Verma, R. P. Mirin, S. W. Nam, K. J. Resch, and T. Jennewein, "Direct generation of three-photon polarization entanglement," Nat. Photonics **8**, 801–807 (2014).
20. M. A. Nielsen, "Optical quantum computation using cluster states," Phys. Rev. Lett. **93**, 040503 (2004).
21. J. Wenger, R. Tualle-Brouri, and P. Grangier, "Non-Gaussian statistics from individual pulses of squeezed light," Phys. Rev. Lett. **92**, 153601 (2004).
22. A. Zavatta, S. Viciani, and M. Bellini, "Quantum-to-classical transition with single-photon-added coherent states of light," Science **306**, 660–662 (2004).
23. V. Parigi, A. Zavatta, M. Kim, and M. Bellini, "Probing quantum commutation rules by addition and subtraction of single photons to/from a light field," Science **317**, 1890–1893 (2007).
24. D. F. Walls, "Squeezed states of light," Nature **306**, 141–146 (1983).
25. D. T. Pegg, L. S. Phillips, and S. M. Barnett, "Optical state truncation by projection synthesis," Phys. Rev. Lett. **81**, 1604–1606 (1998).
26. S. Rosenblum, O. Bechler, I. Shomroni, Y. Lovsky, G. Guendelman, and B. Dayan, "Extraction of a single photon from an optical pulse," Nat. Photonics **10**, 19–22 (2016).
27. S. Rosenblum, A. Borne, and B. Dayan, "Analysis of deterministic swapping of photonic and atomic states through single-photon Raman interaction," Phys. Rev. A **95**, 033814 (2017).
28. O. Bechler, A. Borne, S. Rosenblum, G. Guendelman, O. E. Mor, M. Netser, T. Ohana, Z. Aqua, N. Drucker, R. Finkelstein, Y. Lovsky, R. Bruch, D. Gurovich, E. Shafir, and B. Dayan, "A passive photon-atom qubit swap operation," Nat. Phys. **14**, 996–1000 (2018).
29. D. Pinotsi and A. Imamoglu, "Single photon absorption by a single quantum emitter," Phys. Rev. Lett. **100**, 093603 (2008).
30. G. Lin, X. Zou, X. Lin, and G. Guo, "Heralded quantum memory for single-photon polarization qubits," Europhys. Lett. **86**, 30006 (2009).
31. K. Koshino, S. Ishizaka, and Y. Nakamura, "Deterministic photon-photon swap gate using a Λ system," Phys. Rev. A **82**, 010301 (2010).
32. M. Bradford and J.-T. Shen, "Single-photon frequency conversion by exploiting quantum interference," Phys. Rev. A **85**, 043814 (2012).
33. K. Koshino, K. Inomata, Z. Lin, Y. Tokunaga, T. Yamamoto, and Y. Nakamura, "Theory of deterministic entanglement generation between remote superconducting atoms," Phys. Rev. Appl. **7**, 064006 (2017).
34. I. Shomroni, S. Rosenblum, Y. Lovsky, O. Bechler, G. Guendelman, and B. Dayan, "All-optical routing of single photons by a one-atom switch controlled by a single photon," Science **345**, 903–906 (2014).
35. K. Inomata, K. Koshino, Z. Lin, W. Oliver, J. Tsai, Y. Nakamura, and T. Yamamoto, "Microwave down-conversion with an impedance-matched Λ system in driven circuit QED," Phys. Rev. Lett. **113**, 063604 (2014).
36. K. Inomata, Z. Lin, K. Koshino, W. D. Oliver, J.-S. Tsai, T. Yamamoto, and Y. Nakamura, "Single microwave-photon detector using an artificial Λ-type three-level system," Nat. Commun. **7**, 12303 (2016).
37. R. Lang, M. O. Scully, and W. E. Lamb, Jr., "Why is the laser line so narrow? A theory of single-quasimode laser operation," Phys. Rev. A **7**, 1788–1797 (1973).
38. J. Gea-Banacloche, N. Lu, L. M. Pedrotti, S. Prasad, M. O. Scully, and K. Wódkiewicz, "Treatment of the spectrum of squeezing based on the modes of the universe. I. Theory and a physical picture," Phys. Rev. A **41**, 369–380 (1990).
39. C. Mehta, A. K. Roy, and G. Saxena, "Eigenstates of two-photon annihilation operators," Phys. Rev. A **46**, 1565–1572 (1992).
40. J. Gea-Banacloche and W. Wilson, "Photon subtraction and addition by a three-level atom in an optical cavity," Phys. Rev. A **88**, 033832 (2013).
41. Q. Turchette, R. Thompson, and H. Kimble, "One-dimensional atoms," Appl. Phys. B **60**, S1–S10 (1995).
42. C. Gardiner and M. Collett, "Input and output in damped quantum systems: quantum stochastic differential equations and the master equation," Phys. Rev. A **31**, 3761–3774 (1985).
43. C. Gardiner, "Driving a quantum system with the output field from another driven quantum system," Phys. Rev. Lett. **70**, 2269–2272 (1993).

44. H. Carmichael, "Quantum trajectory theory for cascaded open systems," Phys. Rev. Lett. **70**, 2273–2276 (1993).

45. J. Gea-Banacloche, "Space-time descriptions of quantum fields interacting with optical cavities," Phys. Rev. A **87**, 023832 (2013).

46. S. Rosenblum, S. Parkins, and B. Dayan, "Photon routing in cavity QED: beyond the fundamental limit of photon blockade," Phys. Rev. A **84**, 033854 (2011).

47. M. Um, J. Zhang, D. Lv, Y. Lu, S. An, J.-N. Zhang, H. Nha, M. Kim, and K. Kim, "Phonon arithmetic in a trapped ion system," Nat. Commun. **7**, 11410 (2016).

48. N. Lutkenhaus and S. M. Barnett, "Nonclassical effects in phase space," Phys. Rev. A **51**, 3340–3342 (1995).

49. S. L. Braunstein and A. Mann, "Measurement of the bell operator and quantum teleportation," Phys. Rev. A **51**, R1727–R1730 (1995).

50. J. Tiedau, T. J. Bartley, G. Harder, A. E. Lita, S. W. Nam, T. Gerrits, and C. Silberhorn, "On the scalability of parametric down-conversion for generating higher-order Fock states," arXiv:1901.03237 (2019).

51. N. Somaschi, V. Giesz, L. De Santis, J. Loredo, M. P. Almeida, G. Hornecker, S. L. Portalupi, T. Grange, C. Antón, J. Demory, C. Gómez, I. Sagnes, N. D. Lanzillotti-Kimura, A. Lemaître, A. Auffeves, A. White, L. Lanco, and P. Senellart, "Near-optimal single-photon sources in the solid state," Nat. Photonics **10**, 340–345 (2016).

52. Y.-M. He, J. Liu, S. Maier, M. Emmerling, S. Gerhardt, M. Davanço, K. Srinivasan, C. Schneider, and S. Höfling, "Deterministic implementation of a bright, on-demand single-photon source with near-unity indistinguishability via quantum dot imaging," Optica **4**, 802–808 (2017).

53. R. S. Daveau, K. C. Balram, T. Pregnolato, J. Liu, E. H. Lee, J. D. Song, V. Verma, R. Mirin, S. W. Nam, L. Midolo, S. Stobbe, K. Srinivasan, and P. Lodahl, "Efficient fiber-coupled single-photon source based on quantum dots in a photonic-crystal waveguide," Optica **4**, 178–184 (2017).

54. F. Kaneda, B. G. Christensen, J. J. Wong, H. S. Park, K. T. McCusker, and P. G. Kwiat, "Time-multiplexed heralded single-photon source," Optica **2**, 1010–1013 (2015).

55. A. Jeantet, Y. Chassagneux, C. Raynaud, P. Roussignol, J.-S. Lauret, B. Besga, J. Estève, J. Reichel, and C. Voisin, "Widely tunable single-photon source from a carbon nanotube in the Purcell regime," Phys. Rev. Lett. **116**, 247402 (2016).

56. F. Marsili, V. B. Verma, J. A. Stern, S. Harrington, A. E. Lita, T. Gerrits, I. Vayshenker, B. Baek, M. D. Shaw, R. P. Mirin, and S. W. Nam, "Detecting single infrared photons with 93% system efficiency," Nat. Photonics **7**, 210–214 (2013).

57. M. Arcari, I. Söllner, A. Javadi, S. L. Hansen, S. Mahmoodian, J. Liu, H. Thyrrestrup, E. H. Lee, J. D. Song, S. Stobbe, and P. Lodahl, "Near-unity coupling efficiency of a quantum emitter to a photonic crystal waveguide," Phys. Rev. Lett. **113**, 093603 (2014).

58. X. Ji, F. A. Barbosa, S. P. Roberts, A. Dutt, J. Cardenas, Y. Okawachi, A. Bryant, A. L. Gaeta, and M. Lipson, "Ultra-low-loss on-chip resonators with sub-milliwatt parametric oscillation threshold," Optica **4**, 619–624 (2017).

59. M. H. Pfeiffer, J. Liu, M. Geiselmann, and T. J. Kippenberg, "Coupling ideality of integrated planar high-*Q* microresonators," Phys. Rev. Appl. **7**, 024026 (2017).

60. K. Y. Yang, D. Y. Oh, S. H. Lee, Q.-F. Yang, X. Yi, B. Shen, H. Wang, and K. Vahala, "Bridging ultrahigh-*Q* devices and photonic circuits," Nat. Photonics **12**, 297–302 (2018).

61. A. Borne and B. Dayan, "Deterministic ion-photon qubit exchange in realistic ion cavity-QED systems without strong coupling," arXiv:1902.03469 (2019).

62. M. Davanco, J. Liu, L. Sapienza, C.-Z. Zhang, J. V. D. M. Cardoso, V. Verma, R. Mirin, S. W. Nam, L. Liu, and K. Srinivasan, "Heterogeneous integration for on-chip quantum photonic circuits with single quantum dot devices," Nat. Commun. **8**, 889 (2017).

63. A. Goban, C.-L. Hung, S.-P. Yu, J. Hood, J. Muniz, J. Lee, M. Martin, A. McClung, K. Choi, D. E. Chang, O. Painter, and H. J. Kimble, "Atom-light interactions in photonic crystals," Nat. Commun. **5**, 3808 (2014).